

An experimental study of the effect of fillings on hydraulic properties of single fractures

Richeng Liu¹ · Hongwen Jing¹ · Lixin He¹ · Tantan Zhu¹ · Liyuan Yu¹ · Haijian Su¹

Received: 26 February 2017 / Accepted: 4 October 2017 / Published online: 13 October 2017
© Springer-Verlag GmbH Germany 2017

Abstract Fluid flow in single rock fractures considering the influences of fracture surface roughness, shearing process, normal loading, and so on has been extensively studied for several decades, yet the significant influence of fillings has not been systematically investigated due to the numerous difficulties such as determination of the physical parameters of fillings. The present study aims to estimate the hydraulic properties of single fractures filled with different graded and gap-graded fillings, based on a series of flow tests on rock-like samples using the MTS815.02 material testing system. With the increment of fracture aperture, the pressure drops before and after fillings are flowed away decrease, whereas the permeabilities before and after fillings are flowed away increase. When the ratio of mechanical aperture of fractures to maximum diameter of fillings decreases from 4 to 1.33, both pressure drop and permeability change significantly before the fillings are flowed away and then hold constant values after the fillings are flowed away. Due to the effects of fraction force and interlocking force between particles, the ratio of mechanical aperture to maximum diameter of fillings that equals to 2.67 is the inflection point, where the pressure drop has the maximum value and permeability has the minimum value. When the fractures are filled with gap-graded fillings, in which the ratio of mechanical aperture of fractures to mean diameter of fillings decreases from 5.76 to 1.45, the variations of both pressure drop and permeability before fillings are flowed away change more significantly than those

after fillings are flowed away. The hydraulic aperture of fractures with fillings is approximately 2–3 orders of magnitude smaller than the mechanical aperture.

Keywords Rock fracture · Filling · Material testing system · Permeability · Pressure drop

Introduction

Water leakage and water inrush widely exist in many engineering projects such as the constructions of tunnel, dam, rock slope, and other aspects (Witherspoon et al. 1980; Chen et al. 2000; Cappa et al. 2005; Nazridoust et al. 2006; Crandall et al. 2010; Ferer et al. 2011; Lei et al. 2017). The connected fractures form the main flow paths of fluid within tight rocks, i.e., granite and basalt, in which the rock matrix is assumed impermeable (Leung and Zimmerman 2012; Liu et al. 2016a; Cai et al. 2017a, b). However, the fillings such as clay, sand, and grout are commonly observed in the void space of fractures (Song and Yanful 2010, 2011; Wang et al. 2016) and can significantly affect the hydraulic properties of fractures. Although a large number of studies have focused on fluid flow in rock fractures, the influences of fillings are rarely studied. Therefore, it is necessary to investigate the influences of fillings on the hydraulic properties of rock fractures.

Some previous studies have focused on the influence of fillings on the mechanical and/or hydromechanical behavior of rock joints. For example, Indraratna et al. (2005) proposed a shear strength model to study the shear behavior of idealized infilled joints under constant normal stiffness conditions. They found that the combined effect of basic fraction angle and joint asperity angle is firstly

✉ Hongwen Jing
hwjingcumt@126.com

¹ State Key Laboratory for Geomechanics and Deep Underground Engineering, China University of Mining and Technology, Xuzhou 221116, People's Republic of China

pronounced and then diminished with increasing the ratio of infill thickness to asperity height of joints. The proposed new model is capable of describing the shear behaviors of the graphite and clay (bentonite)-filled rock joints. Indraratna et al. (2008) later conducted a series of experimental tests to address the effect of the overconsolidation of infilled rough joints on undrained shear behavior, in which the idealized sawtoothed joints are filled with natural silty clay. The results showed that asperity plays a significant role on shear strength up to a critical ratio of asperity height to infill thickness; however, when beyond the critical ratio, the shear is controlled by the infill alone. Wu et al. (2014) investigated the role of fillings (i.e., quartz sand and kaolin clay) in the interaction between a P-wave and a rock fracture by conducting a series of experiments on rock fractures filled with pure quartz sand, sand–clay mixtures, and a pure clay matrix. They found that fracture stiffness and wave transmission coefficient decrease with the increment of filling material thickness, and the filled fracture exhibits the largest fracture stiffness when the void space of quartz sand is completely filled with clay matrix. Rutqvist (2015) reviewed field data on stress-induced permeability changes in fractured rock masses, in which the influences of in situ conditions such as fracture shear offset and fracture infilling by mineral precipitation on the stress–permeability relationship of fractured rock masses were illustrated. Gui et al. (2016) used hybrid continuum-discrete element method to simulate P-wave propagation in rock masses containing granular material-filled fractures. They concluded that the non-welded fracture containing filling materials provides the highest attenuation factor, whereas the welded fracture that does not contain filling materials attenuates the least energy. Khosravi et al. (2016) presented a new testing device to estimate the hydromechanical behaviors of infilled rock fractures in an unsaturated state and reported that when rock fracture is filled with compacted silt, the shear strength increases during drying. Besides, the thickness of fracture has a significant influence on the shear strength of the infilled rock fracture. However, the above studies did not consider the role of the spilling of fillings, which can change the magnitudes of both pressure drop and permeability, during the experiments and/or simulations.

The present study aims to investigate the hydraulic behaviors (i.e., the variations of pressure drop and permeability) of rock-like joints filled with materials having different levels of grading and different fracture apertures. “Theoretical background” section presents the theoretical background for fluid flow in rock fractures. “Testing system” section prepares a series of rock-like samples containing fillings and conducts flow tests on the MTS815.02

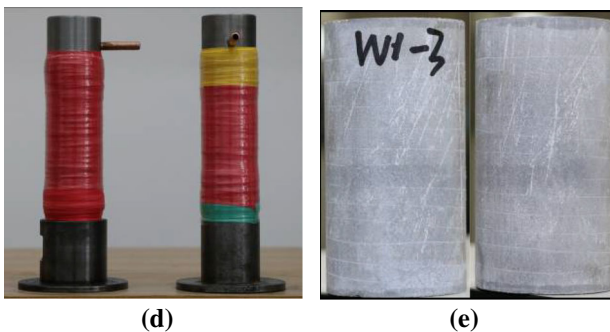
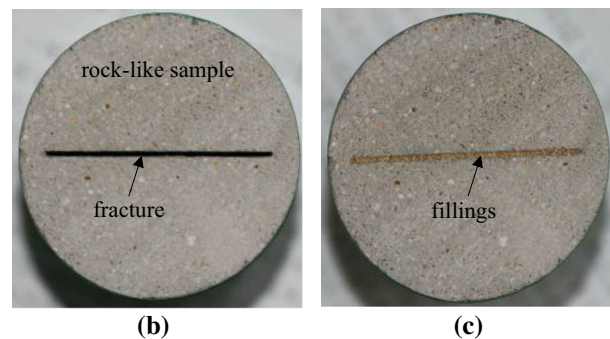
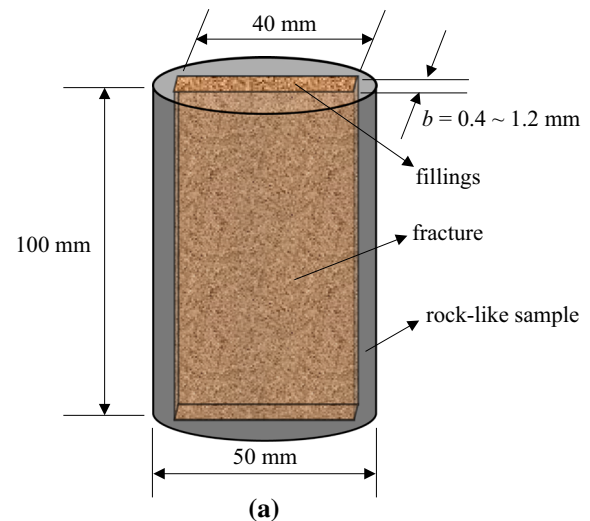


Fig. 1 Schematic view of a sample and rock-like samples before and after fillings. **a** Schematic view of a sample containing a fracture with fillings. **b** Top view of rock-like sample without fillings. **c** Top view of rock-like sample with fillings. **d** Sealing of rock-like samples. **e** Rock-like samples after flow tests

testing system. “Results and analysis” section analyzes the effects of fracture aperture, graded, and gap-graded fillings on the hydraulic properties of rock fractures such as pressure drop, permeability change, and the ratio of hydraulic aperture to mechanical aperture. Finally, “Conclusions” section summarizes the obtained main conclusions.

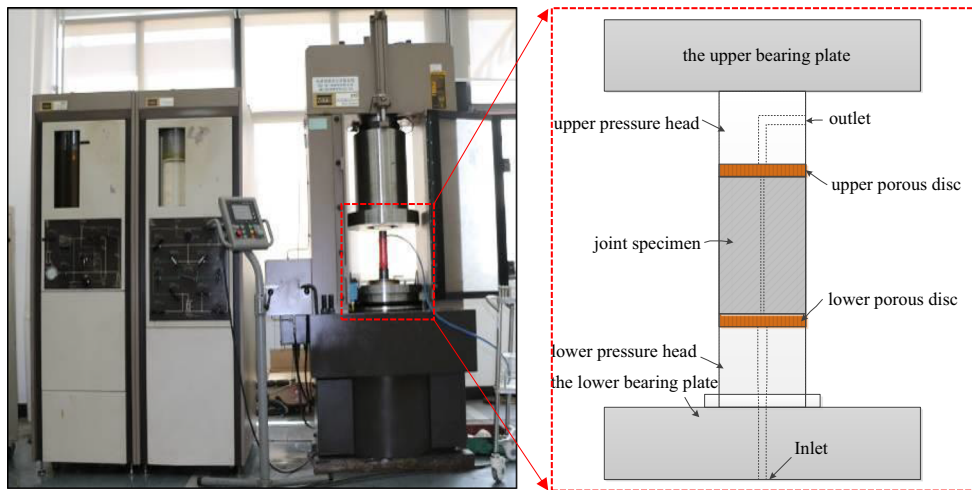


Fig. 2 MTS815.02 testing system and enlarged schematic view of flow system

Table 1 Three experimental cases and corresponding parameters

Case no.	q (mm ³ /s)	b (mm)	D_m (mm)	D_g (mm)	b/D_m	b/D_g
1	981.75	0.4	0.2	–	2	–
		0.6	0.2	–	3	–
		0.8	0.2	–	4	–
		1.0	0.2	–	5	–
		1.2	0.2	–	6	–
2	981.75	0.8	0.2	–	4	–
		0.8	0.3	–	2.67	–
		0.8	0.4	–	2	–
		0.8	0.5	–	1.6	–
		0.8	0.6	–	1.33	–
3	981.75	0.8	–	0.14	–	5.76
		0.8	–	0.24	–	3.34
		0.8	–	0.35	–	2.29
		0.8	–	0.45	–	1.78
		0.8	–	0.55	–	1.45

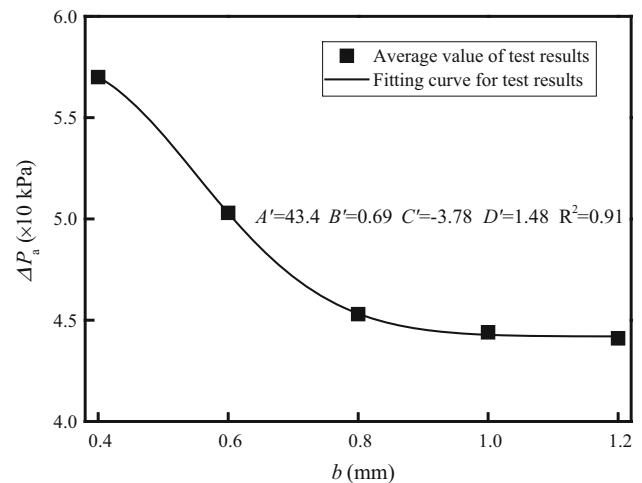


Fig. 4 Relationships between ΔP_a and b

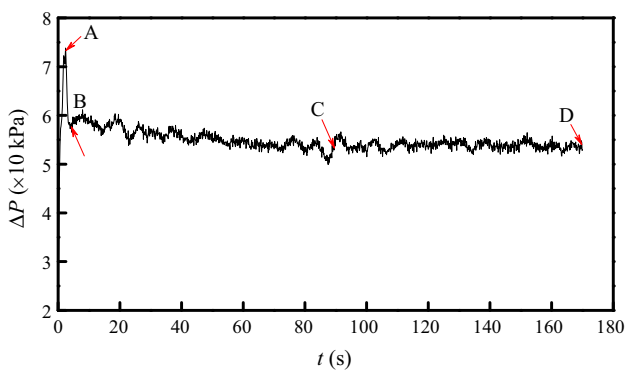


Fig. 3 Variations of pressure drop over time

Theoretical background

Fluid flow in rock fractures with sufficiently low flow rate obeys the cubic law, written as (Bear 1972; Zimmerman and Bodvarsson 1996; Yeo et al. 1998; Liu et al. 2016b, c):

$$Q = \frac{we^3 \Delta P}{12\mu L} \tag{1}$$

where Q is the flow rate, e is the hydraulic aperture, μ is the dynamic viscosity, w is the fracture width, P is the pressure, and L is the fracture length.

However, the cubic law is only applicable for fractures consisting of two ideal smooth parallel plates (Chen et al. 2015). When the fracture surface is rough or the void space is filled with fillings, the cubic law is not applicable. Considering that the hydraulic gradient J is defined as the

Table 2 Test results of hydraulic properties for samples in Case 1

b/D_m	ΔP_m ($\times 10$ kPa)	ΔP_a ($\times 10$ kPa)	K_{f1} ($\times 10^{-6}$ mm ²)	K_{f2} ($\times 10^{-6}$ mm ²)	p_1	k_1
2	8.31	5.71	0.60	0.88	0.69	1.46
3	7.40	5.04	0.68	0.99	0.68	1.47
4	6.76	4.54	0.75	1.10	0.67	1.47
5	5.78	4.46	0.82	1.12	0.73	1.36
6	5.53	4.42	0.95	1.13	0.84	1.19

ratio of hydraulic head difference applied at the two tips of a fracture to fracture length, Eq. (1) can be rewritten as:

$$Q = w \frac{\rho g e^3}{12\mu} J \quad (2)$$

where ρ is the fluid density and g is the gravitational acceleration.

For a laminar flow, many researchers, such as Lomize (1951), Louis (1969), Su et al. (1995), Barton et al. (1985), and Xiong et al. (2011), have corrected the cubic law taking into account the influences of fracture surface roughness and aperture variation, as shown in the following Eqs. (3)–(7).

$$Q = w \frac{\rho g (\bar{b})^3}{12\mu} J \frac{1}{1 + 6 \left(\frac{\Delta}{\bar{b}}\right)^{1.5}} \quad (3)$$

$$Q = w \frac{\rho g (\bar{b})^3}{12\mu} J \frac{1}{1 + 8.8 \left(\frac{\Delta}{2\bar{b}}\right)^{1.5}} \quad (4)$$

$$Q = w \frac{\rho g (\bar{b})^3}{12\mu} J \frac{1}{1 + 1.2 \left(\frac{\Delta}{2\bar{b}}\right)^{-0.75}} \quad (5)$$

$$Q = w \frac{\rho g (\bar{b})^3}{12\mu} J \frac{1}{1 + 0.6 \left(\frac{\sigma_{\text{apert}}}{2\bar{b}}\right)^{1.2}} \quad (6)$$

$$Q = w \frac{\rho g}{12\mu} J b^3 \left(1 - 1.0 \frac{\sigma_{\text{apert}}}{b}\right) \left(1 - \frac{\sigma_{\text{apert}}}{b} \frac{\sqrt{\sigma_{\text{slope}}}}{10} \sqrt{Re}\right) \quad (7)$$

where b is the mechanical aperture, \bar{b} is the mean mechanical aperture, Δ is the roughness of joint, σ_{apert} is the standard deviation of mean mechanical aperture, σ_{slope} is the standard deviation of local slope of fracture surface, and Re is the Reynolds number. Some other works that present the empirical expressions for hydraulic aperture are summarized and described in Li et al. (2016). However, the modified cubic law cannot be utilized to simulate fluid flow in fractures filled with fillings, because the incompressible Newtonian fluid in steady-state flow obeys the Hagen–

Poiseuille equation. Therefore, some new expressions are needed to model flow in fractures filled with fillings.

Testing system

Specimen preparation

The rock-like material such as the cement mortar was selected for specimen preparation, due to its more excellent homogeneity, comparing with natural rocks (Cheng et al. 2016). The rock-like samples were made by mixing quarts sand, cement, and water with a ratio of 1:1:0.6, in which the quarts sand was filtrated using a square mesh sieve with a mesh length of 1 mm from the natural river sands. The cement was the Portland cement of P.O.32.5. The rock-like samples were poured using a high-strength acrylic mold with an inner diameter of 50 mm and a length of 100 mm, as shown in Fig. 1a. A stainless steel with a size of 100 \times 40 mm, which was wiped using lubricating oil, was fixed at the middle of the acrylic mold using two silicon pads before pouring. The thickness of the stainless steel can be changed according to the requirements. After pouring, samples were processed by vibrating, mold release, maintenance, cutting, and grinding, respectively. Then, the stainless steel was slowly drawn out, and the intersection between samples and stainless steel was constantly rinsed using water until there are no lubrication oils left. The top view of the prepared rock-like sample is shown in Fig. 1b. Next, fillings that were selected using square mesh sieve with different mesh sizes were put into the fractures as shown in Fig. 1c. Finally, the samples were packaged by adding an upper pressure head, an upper porous disk, a lower porous disk, and a lower pressure head and were sealed using four layers of PVC tapes and three layers of hear shrink tubes. The samples after sealing are presented in Fig. 1d. Figure 1e exhibits two samples after flow tests, which shows that only the edges are wet and indicates that the sealing treatment performs well. The density of the rock-like samples is 1.95 g/cm³, and the density of the fillings is in the range of 0.90–1.56 g/cm³ according to the maximum diameter of the quarts sand.

Testing unit

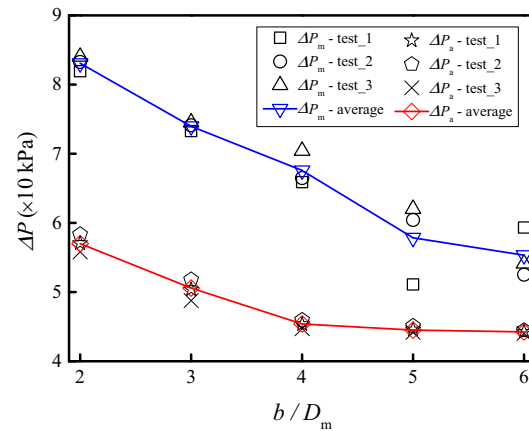
The MTS815.02 material testing system with a maximum loading capacity of 1700 kN was firstly utilized to test the hydraulic properties through a self-made water flow device (see Fig. 2). An inlet was installed in the lower pressure head, and an outlet was installed in the upper pressure head. The fluid flows from the pore water pressure load system, to the one-way valve, to the specimen, to the outlet, and to a collector. The water flow rate can be controlled constant using this pore water pressure load system. The pressure between the inlet and the outlet was measured using a pressure gauge. The controller that includes a distributor, a computer, and software was utilized to collect and analyze the data.

Testing procedure

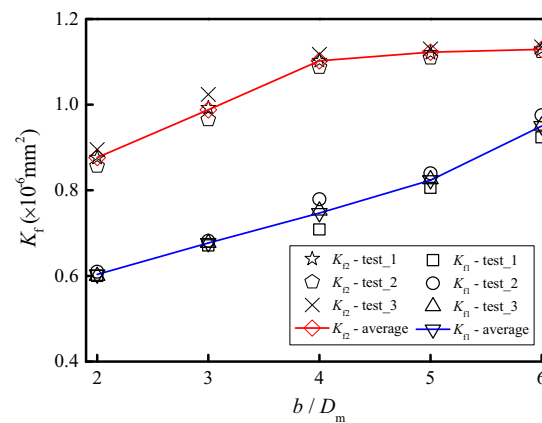
To investigate the influence of fractures filled with materials having different levels of grading and different fracture apertures on the hydraulic behaviors of rock-like samples, three cases were considered for the flow tests. The details of the three cases are illustrated in Table 1.

In Case 1, fracture aperture (b) varies from 0.4 to 1.2 mm at an interval of 0.2 mm, and the filling materials are quarts sand that is well graded with the largest diameter (D_m) of 0.2 mm. In Case 2, b is fixed at 0.8 mm, and the filling materials are quarts sand that is well graded with $D_m = 0.2, 0.3, 0.4, 0.5,$ and 0.6 mm, respectively. In Case 3, b is fixed at 0.8 mm, and the filling materials are quarts sand that is gap graded. Five rock-like samples are prepared and the diameter of their fillings is in the range 0.1–0.2, 0.2–0.3, 0.3–0.4, 0.4–0.5, and 0.5–0.6 mm, respectively. Their mean diameters (D_g) are 0.14, 0.24, 0.35, 0.45, and 0.55 mm, respectively.

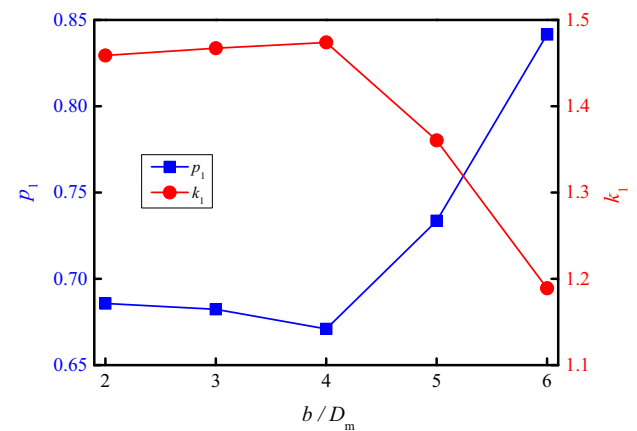
When a rock-like sample is prepared and the fracture is filled with fillings, it will be sealed and then put into the MTS815.02 testing system. All the valves connected to the inlet and outlet are opened, and a constant flow rate of $981.75 \text{ mm}^3/\text{s}$ is injected into the model through the pore water pressure load system. Simultaneously, the pressure drop obtained from the pressure gauge is recorded. When the flow is in a steady state, in which the pressure drop holds a constant value, the test is completed (i.e., the point D in Fig. 3). Here, an assumption is made that there are no clays and/or organic materials in the fillings.



(a) Relationships between ΔP and b/D_m



(b) Relationships between K_f and b/D_m



(c) Variations of p_1 and k_1 with varying b/D_m

Fig. 5 Variations of a ΔP , b K_f , c p_1 and k_1 , with varying b/D_m from 2 to 6 for Case 1

Table 3 Test results of hydraulic properties for samples in Case 2

b/D_m	ΔP_m ($\times 10$ kPa)	ΔP_a ($\times 10$ kPa)	K_{f1} ($\times 10^{-6}$ mm^2)	K_{f2} ($\times 10^{-6}$ mm^2)	p_1	k_1
4.00	6.77	4.55	0.74	1.11	0.67	1.50
2.67	17.48	4.61	0.29	1.14	0.26	3.88
2.00	13.82	4.46	0.36	1.14	0.32	3.12
1.60	10.31	4.35	0.50	1.18	0.42	2.32
1.33	6.06	4.84	0.84	1.04	0.80	1.24

Results and analysis

Effect of aperture

In the Case 1, fracture aperture changes from 0.4 to 1.2 mm. When the flow becomes steady, the measured pressure drop is recorded. Figure 4 shows the relationship between pressure drop and aperture. The results show that with the increment of aperture, the pressure drop decreases first significantly and then gently. By fitting the tested results, a new expression is proposed, written as:

$$\Delta P = \left\{ \frac{12\mu Q \left[1 + A' \left(\frac{b'}{b} \right)^{C'} \right]}{(\rho g)^{D'+1} b^4} \right\}^{\frac{1}{D'}} \tag{8}$$

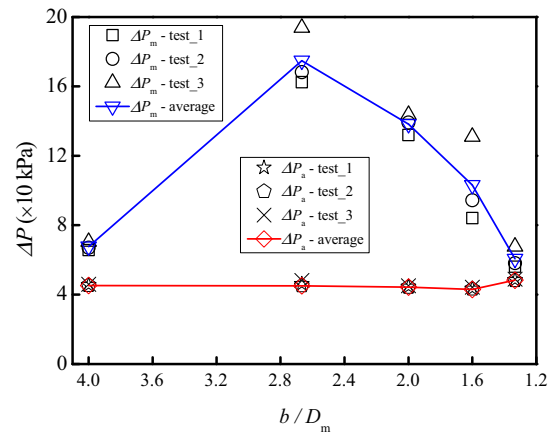
where A' , B' , C' , and D' are coefficients that are related to the geometries of fracture and parameters of filling materials. In the present study, $A' = 43.4$, $B' = 0.69$, $C' = -3.78$, and $D' = 1.48$. The correlation coefficient $R^2 = 0.91$, indicating that Eq. (8) is suitable for describing the relationship between pressure drop and aperture for the specimens presented. However, its applicability for other cases needs to be deeply studied.

The permeability is a parameter that is widely used for characterizations of fluid flow in fractures, which can be back-calculated from the linear Darcy’s law, written as:

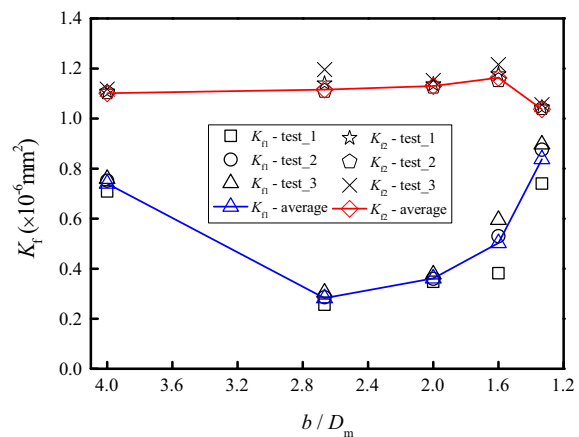
$$K_f = \frac{Q\mu L}{A\Delta P} \tag{9}$$

where K_f is the permeability.

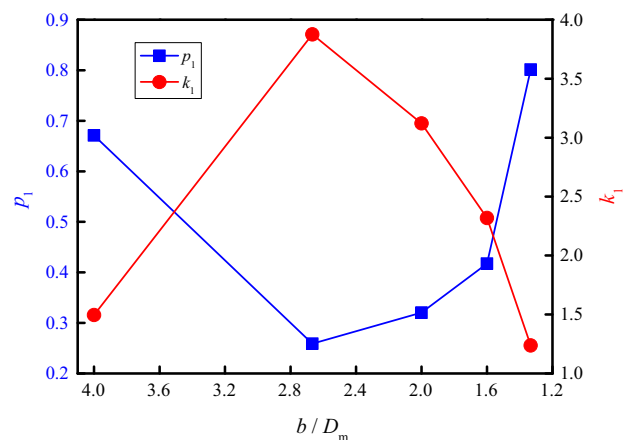
Since some of the filling materials with a small particle size can spill from the samples, the mean aperture increases and the pressure drop decreases as shown in Fig. 3. The maximum pressure drop such as point A represents the pressure drop, in which no fillings flow always along with fluid flow. The constant pressure drop such as point D illustrates the pressure drop, in which some fillings have flowed away and the flow is steady. As a result, the permeability corresponding to point D would be much larger



(a) Relationships between ΔP and b/D_m



(b) Relationships between K_f and b/D_m



(c) Variations of p_1 and k_1 with varying b/D_m

Fig. 6 Variations of **a** ΔP , **b** K_f , **c** p_1 and k_1 , with varying b/D_m from 1.33 to 4 for Case 2

than that corresponding to point A, because some sands are spilled from the model. To characterize the two pressure drops, as well as their corresponding permeabilities, the following two expressions are defined:

Table 4 Test results of hydraulic properties for samples in Case 3

b/D_g	ΔP_m ($\times 10$ kPa)	ΔP_a ($\times 10$ kPa)	K_{f1} ($\times 10^{-6}$ mm ²)	K_{f2} ($\times 10^{-6}$ mm ²)	p_1	k_1
5.76	29.06	4.59	0.17	1.09	0.16	6.26
3.34	19.04	4.66	0.26	1.08	0.24	4.09
2.29	15.73	4.99	0.32	1.01	0.32	3.13
1.78	9.18	5.37	0.56	0.93	0.58	1.66
1.45	7.15	5.83	0.70	0.82	0.86	1.15

$$K_{f1} = \frac{Q\mu L}{A\Delta P_m} \tag{10}$$

$$K_{f2} = \frac{Q\mu L}{A\Delta P_a} \tag{11}$$

where ΔP_m is the maximum pressure drop, K_{f1} is the corresponding permeability, ΔP_a is the steady-state pressure drop, and K_{f2} is the corresponding permeability.

For each case, three rock-like samples were manufactured and the mean parameters such as K_{f1} , K_{f2} , ΔP_m , and ΔP_a were calculated. Table 2 and Fig. 5a show the variations of pressure drop with varying b/D_m from 2 to 6. With the increment of b/D_m , ΔP_a decreases dramatically and then gently. When b/D_m increases from 2 to 4, ΔP_a decreases from 5.71×10^{-2} to 4.54×10^{-2} MPa in a rate of 20.49%. When b/D_m increases from 4 to 6, ΔP_a decreases from 4.54×10^{-2} to 4.42×10^{-2} MPa in a rate of 2.64%. However, ΔP_m decreases continuously from 8.31×10^{-2} to 5.53×10^{-2} MPa in a rate of 33.45% and following approximate linear functions. As shown in Fig. 5b with the increment of b/D_m , both K_{f1} and K_{f2} increase and K_{f2} is larger than K_{f1} . When $b/D_m < 4$, the increase rate of K_{f2} is larger than that of K_{f1} , whereas when $b/D_m > 4$, the increase rate of K_{f2} is smaller than that of K_{f1} . Therefore, there is an inflection point, in which $b/D_m = 4$, indicating that the aperture (0.8 mm) is four times larger than the maximum diameter of fillings (0.2 mm).

With the increasing b/D_m , K_{f1} increases linearly and can be fitted using the following expression, written as:

$$K_{f1} = mb/D_m + n \tag{12}$$

where m and n are two coefficients related to the geometric parameters of both fracture and rock. Substituting Eq. (12) into Eq. (10) yields:

$$\Delta P_m = \frac{Q\mu L}{A(mb/D_m + n)} \tag{13}$$

When there are no fractures in an intact rock, $b/D_m = 0$ and Eqs. (12) and (13) can be simplified as:

$$K_{f1} = n \tag{14}$$

$$\Delta P_m = \frac{Q\mu L}{An} \tag{15}$$

Therefore, n is the permeability of rock matrix and has no correlations with the fracture properties such as aperture, length, and roughness. Differentiating Eq. (12) with respect to b/D_m gives:

$$\frac{dK_{f1}}{d(b/D_m)} = m \tag{16}$$

Equation (16) implies that m is a coefficient that describes the sensitivity of K_{f1} with respect to b/D_m . The larger m indicates that K_{f1} is more sensitive to b/D_m . With the same increment of b/D_m , K_{f1} increases more significantly with a larger m . To characterize the hydraulic properties of fractures before and after the fillings are flowed away, the relative pressure drop p_1 and the relative permeability k_1 are defined as:

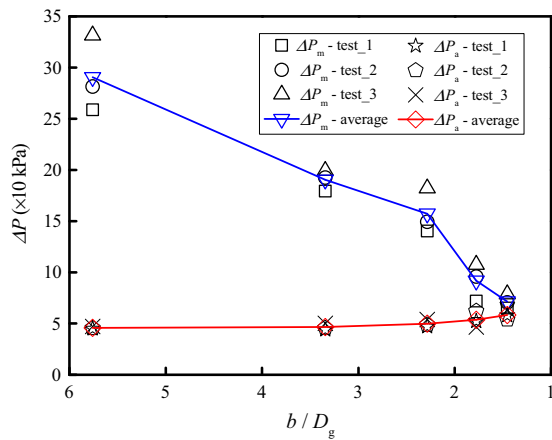
$$p_1 = \frac{\Delta P_a}{\Delta P_m} \tag{17}$$

$$k_1 = \frac{K_{f1}}{K_{f2}} \tag{18}$$

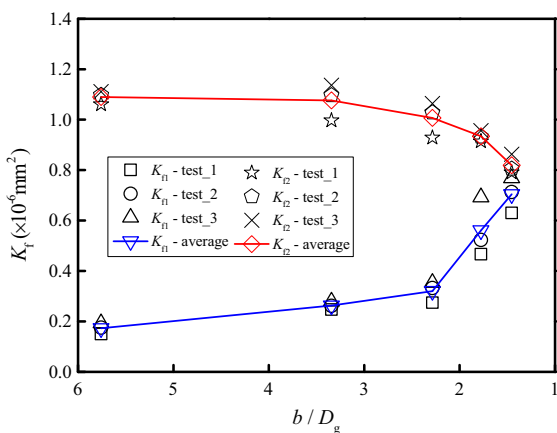
The variations of p_1 and k_1 with the increase in b/D_m are described in Fig. 5c, showing a two-stage property. At the first stage with $b/D_m = 2-4$, p_1 decreases from 0.69 to 0.67 in a rate of 2.90% and k_1 increases from 1.46 to 1.47 in a rate of 0.68%. The reason is that both the decrease rates of ΔP_m and ΔP_a and the increase rates of K_{f1} and K_{f2} are almost the same when $b/D_m < 4$, resulting in that their ratios (p_1 and k_1) hold constant values with the increment of b/D_m . At the second stage with $b/D_m = 4-6$, p_1 increases from 0.67 to 0.84 in a rate of 25.37% and k_1 decreases from 1.47 to 1.19 in a rate of 19.05%. This is because that at this stage, ΔP_a and K_{f2} hold approximate constant values, yet both ΔP_m and K_{f1} change dramatically. Therefore, p_1 and k_1 more significantly depend on a larger b/D_m .

Effect of graded fillings

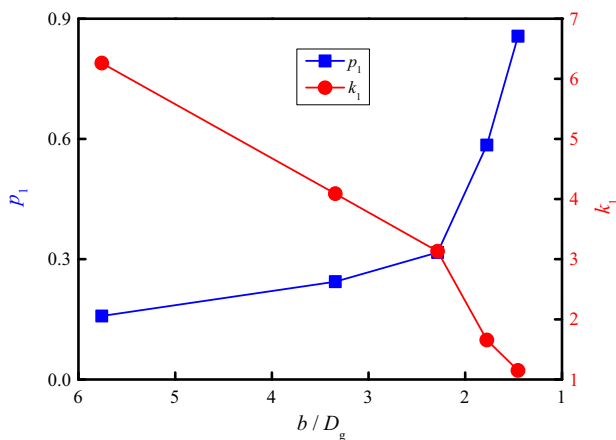
In the Case 2, fracture aperture is fixed at 0.8 mm and fractures are filled with quartz sand that is well graded with b/D_m decreasing from 4 to 1.33 as shown in Table 1. As b/D_m decreases from 4 to 2.67, ΔP_m increases from 6.77×10^{-2} to 17.48×10^{-2} MPa in a rate of 158.20% and then decreases from 17.48×10^{-2} to



(a) Relationships between ΔP and b/D_g



(b) Relationships between K_f and b/D_g



(c) Variations of p_1 and k_1 with varying b/D_g

Fig. 7 Variations of **a** ΔP , **b** K_f , **c** p_1 and k_1 , with varying b/D_g from 1.45 to 5.76 for Case 3

6.06×10^{-2} MPa in a rate of 65.33% for b/D_m decreasing from 2.67 to 1.33 as shown in Table 3 and Fig. 6a. For $b/D_m = 1.33-4$, the maximum and minimum values of ΔP_a are 4.84×10^{-2} and 4.35×10^{-2} MPa, respectively, with

a difference of 10.33%. Figure 6b shows the variations of K_{f1} and K_{f2} . With the decrement of b/D_m from 4 to 2.67, K_{f1} decreases from 0.74×10^{-6} to 0.29×10^{-6} mm² in a rate of 60.81% and then increases from 0.29×10^{-6} to 0.84×10^{-6} mm² in a rate of 60.81%. For $b/D_m = 1.33-4$, the maximum and minimum values of K_{f2} are 1.18×10^{-6} and 1.04×10^{-6} mm², respectively, with a difference of 11.86%. The b/D_m has a robust influence on the hydraulic properties (i.e., ΔP_m and K_{f1}) before some of the fillings flow away, but plays a negligible role on the hydraulic properties (i.e., ΔP_a and K_{f2}) after some of the fillings flow away. The reasons are that when $b/D_m = 4$, both the friction force and interlocking force between particles are very small and the fillings can be easily flowed away. With the decrement of b/D_m by up to 2.67, both the friction force and interlocking force between particles increase and the fillings become more difficult to flow away. When b/D_m is smaller than 2.67, the smaller particle exhibits a stronger reunion effect according to the theory of classical continuous size particle accumulation. As a result, ΔP_m dramatically decreases and K_{f1} significantly increases as b/D_m increases.

Figure 6c exhibits the influences of b/D_m on both p_1 and k_1 . With the decreasing b/D_m from 4 to 2.67, p_1 decreases from 0.67 to 0.26 in a rate of 61.19% and k_1 increases from 1.50 to 3.88 in a rate of 158.66%. With the continuous decrease in b/D_m from 2.67 to 1.33, p_1 increases from 0.26 to 0.80 in a rate of 207.69% and k_1 decreases from 3.88 to 1.24 in a rate of 68.04%. This again verifies that the inflection point locates at $b/D_m = 2.67$, which indicates that in such a case the fillings are more possible to flow away, comparing with other cases.

Effect of gap-graded fillings

In the Case 3, fracture aperture is fixed at 0.8 mm, and the filling materials are quarts sand that is gap graded with $b/D_g = 1.45, 1.78, 2.29, 3.34, \text{ and } 5.76$, respectively. Table 4 and Fig. 7a show that for b/D_g decreasing from 5.76 to 1.45, ΔP_m decreases from 29.06×10^{-2} to 7.15×10^{-2} MPa in a rate of 75.40%, and ΔP_a increases from 4.59×10^{-2} to 5.83×10^{-2} MPa in a rate of 27.02%. K_{f1} increases from 0.17×10^{-6} to 0.70×10^{-6} mm² in a rate of 311.76%, and K_{f2} decreases from 1.09×10^{-6} to 0.82×10^{-6} mm² in a rate of 24.77%. The variation trends for both pressure drop and permeability before fillings are flowed away are different with those after fillings are flowed away. The reasons may be that the void space of fractures before fillings are flowed away can be better filled with quarts sand having a smaller b/D_g and the equivalent hydraulic aperture is consequently smaller, which results in a lower pressure drop (ΔP_m) and a larger permeability (K_{f1}). However, after the fillings are

Table 5 Variations of e/b for all cases

Case 1			Case 2			Case 3		
b/D_m	$e_1/b (\times 10^{-3})$	$e_2/b (\times 10^{-3})$	b/D_m	$e_1/b (\times 10^{-3})$	$e_2/b (\times 10^{-3})$	b/D_g	$e_1/b (\times 10^{-3})$	$e_2/b (\times 10^{-3})$
2	8.11	6.71	4.00	4.54	3.73	5.76	4.52	1.80
3	5.74	4.75	2.67	4.57	2.32	3.34	4.50	2.22
4	4.55	3.76	2.00	4.60	2.60	2.29	4.35	2.45
5	3.67	3.15	1.60	4.67	3.07	1.78	4.19	3.24
6	3.07	2.82	1.33	4.41	3.96	1.45	3.92	3.63

flowed away, the fillings with larger b/D_g are more possible to be left within the fractures, which gives rise to a higher pressure drop (ΔP_a) and a smaller permeability (K_{f2}).

Figure 7c depicts the variations of p_1 and k_1 with $b/D_g = 1.45\text{--}5.76$ mm. With the decrement of b/D_g , p_1 increases from 0.16 to 0.86 in a rate of 437.50% and the increasing rate is stronger for a larger b/D_g , whereas k_1 decreases from 6.26 to 1.15 in a rate of 81.63% and the decreasing rate is weaker for a larger b/D_g .

Evolution of hydraulic aperture

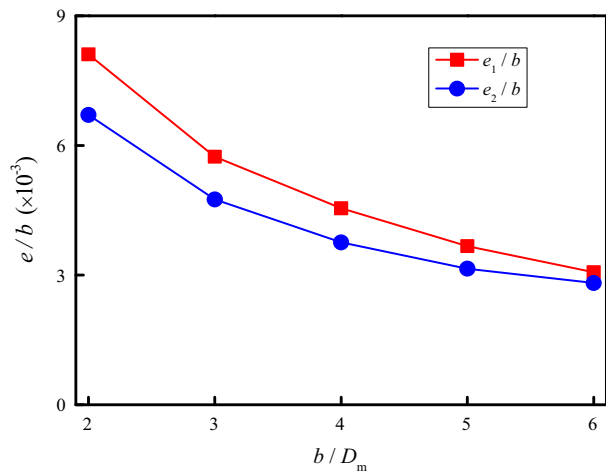
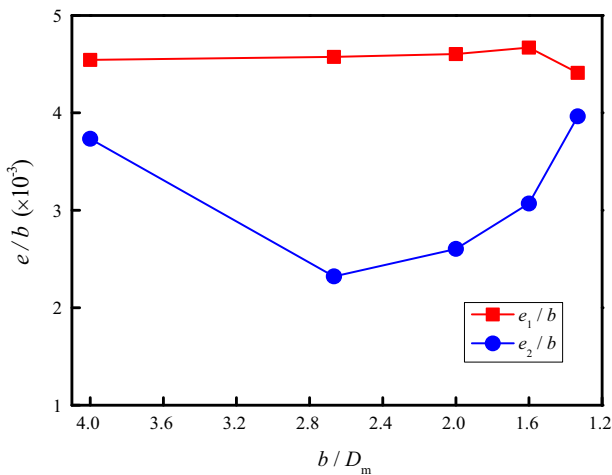
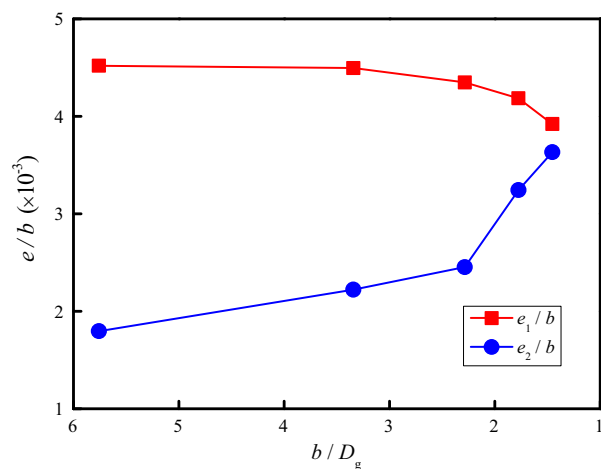
To investigate the roles of fracture surface roughness and contact ratio, the hydraulic aperture (e) is commonly calculated according to the cubic law, and the ratio of hydraulic aperture to mechanical aperture (b/e) has been extensively studied in previous works (Patir and Cheng 1978; Walsh 1981; Zimmerman and Bodvarsson 1996; Olsson and Barton 2001; Rasouli and Hosseinian 2011). In the present study, we calculated the hydraulic apertures before and after the fillings are flowed away, which are represented by e_1 and e_2 , respectively. The influences of b/D_m and b/D_g on the evolution of e/b are exhibited in Table 5 and Fig. 8. For Case 1, with the increment of b/D_m from 2 to 6, e_1/b decreases from 8.11×10^{-3} to 3.07×10^{-3} in a rate of 62.15% and e_2/b decreases from 6.71×10^{-3} to 2.82×10^{-3} in a rate of 57.97%. For Case 2, when b/D_m decreases from 4 to 1.6, e_1/b increases from 4.54×10^{-3} to 4.67×10^{-3} in a rate of 2.86% and then decreases from 4.67×10^{-3} to 4.41×10^{-3} in a rate of 5.57% as b/D_m decreases from 1.6 to 1.33. However, the evolution of e_2/b is very different with that of e_1/b . The value of e_2/b decreases from 3.73×10^{-3} to 2.32×10^{-3} in a rate of 37.80% for b/D_m decreasing from 4 to 2.67 and then increases from 2.32×10^{-3} to 3.96×10^{-3} in a rate of 41.41% for D_m decreasing from 2.67 to 1.33. With the decreasing b/D_g from 5.76 to 1.45, e_1/b continuously decreases from 4.52×10^{-3} to 3.92×10^{-3} in a rate of 13.27%, whereas e_2/b continuously increases from 1.80×10^{-3} to 3.63×10^{-3} in a rate of 101.67%. The reasons are that the larger b/D_g results in that it is easier to construct the fillings in the void space of fractures and the

fillings are more difficult to flow away; therefore, e_1/b continuously decreases and e_2/b continuously increases.

Conclusions

This study focuses on the roles of fillings on the hydraulic properties of fractured rock-like samples. A series of rock-like samples with different fracture apertures, graded, and gap-graded fillings were prepared, and flow tests using the MTS815.02 material testing system were conducted. The influences of fracture aperture, maximum diameter of the graded filling materials, mean diameter of the gap-graded filling materials, and evolution of hydraulic aperture were systematically estimated.

The results show that a new expression for describing fluid flow in fractures filled with fillings is proposed. When the fractures are filled with well-graded fillings having a maximum diameter of 0.2 mm, an inflection point that corresponds to an aperture of 0.8 mm exists, before which both pressure drop and permeability change significantly against the increase in aperture and after which both pressure drop and permeability hold almost constant values. Both the permeabilities before and after the fillings flow away increase with the increment of aperture. When the fractures are well graded with fillings, in which the ratio of mechanical aperture to the maximum diameter decreases from 4 to 1.33, it is found that the pressure drop has a maximum value and permeability has a minimum value when the ratio of mechanical aperture to the maximum diameter = 2.67. This is because when the ratio of mechanical aperture to the maximum diameter decreases from 4 to 2.67, both the friction force and interlocking force between particles are very small and the fillings can be easily flowed away. When the ratio of mechanical aperture to the maximum diameter is smaller than 2.67, the smaller particle exhibits a stronger reunion effect according to the theory of classical continuous size particle accumulation. As a result, the pressure drop and permeability before the fillings are flowed away dramatically decrease and significantly increase, respectively. When the fractures are filled with gap-graded fillings, in which the ratio of

(a) Relationships between e/b and b/D_m for Case 1(b) Relationships between e/b and b/D_m for Case 2(c) Relationships between e/b and b/D_g for Case 3**Fig. 8** Variations of e/b with different **a** b , **b** b/D_m , and **c** b/D_g

mechanical aperture of fractures to mean diameter of fillings varies from 1.45 to 5.76, the pressure drop before the fillings are flowed away changes more robustly than that after the fillings are flowed away, and the permeability change shows very different trends. The reasons may be that before the fillings are flowed away, the void space of fractures is better filled with quartz sand having a smaller mean diameter. As a result, the equivalent aperture is smaller, and the permeability is larger. After some of the fillings are flowed away, the fillings with a larger mean diameter are more possible to be left within the fractures, and the permeability is smaller. The variations of ratio of hydraulic aperture to mechanical aperture are similar to those of permeability change, because according to Darcy's law, the hydraulic aperture is linearly proportional to the square root of permeability.

The future works will be focused on the influences of confining pressure applied on the samples, the fracture surface roughness, and shearing process on the hydraulic properties of fractures, which are not considered in this study.

Acknowledgements This study has been partially funded by National Basic Research 973 Program of China, China (Grant No. 2013CB036003), and National Natural Science Foundation of China, China (Grant Nos. 51579239, 51374198, 51323004). These supports are gratefully acknowledged.

References

- Barton N, Bandis S, Bakhtar K (1985) Strength, deformation and conductivity coupling of rock joints. *Int J Rock Mech Min Sci* 22(3):121–140
- Bear J (1972) Dynamics of fluids in porous media. Elsevier, New York
- Cai J, Wei W, Hu X, Liu R, Wang J (2017a) Fractal characterization of dynamic fracture network extension in porous media. *Fractals* 25(02):1750023
- Cai J, Wei W, Hu X, Wood DA (2017b) Electrical conductivity models in saturated porous media: a review. *Earth-Sci Rev* 171:419–433
- Cappa F, Guglielmi Y, Fénart P, Merrien-Soukatchoff V, Thoraval A (2005) Hydromechanical interactions in a fractured carbonate reservoir inferred from hydraulic and mechanical measurements. *Int J Rock Mech Min Sci* 42(2):287–306
- Chen Z, Narayan SP, Yang Z, Rahman SS (2000) An experimental investigation of hydraulic behaviour of fractures and joints in granitic rock. *Int J Rock Mech Min Sci* 37(7):1061–1071
- Chen YF, Zhou JQ, Hu SH, Hu R, Zhou CB (2015) Evaluation of Forchheimer equation coefficients for non-Darcy flow in deformable rough-walled fractures. *J Hydrol* 529:993–1006
- Cheng H, Zhou X, Zhu J, Qian Q (2016) The effects of crack openings on crack initiation, propagation and coalescence behavior in rock-like materials under uniaxial compression. *Rock Mech Rock Eng* 49(9):3481–3494
- Crandall D, Ahmadi G, Smith DH (2010) Computational modeling of fluid flow through a fracture in permeable rock. *Transp Porous Med* 84(2):493–510

- Ferer M, Crandall D, Ahmadi G, Smith DH (2011) Two-phase flow in a rough fracture: experiment and modeling. *Phys Rev E* 84(1):016316
- Gui YL, Zhao ZY, Zhou HY, Wu W (2016) Numerical simulation of P-wave propagation in rock mass with granular material-filled fractures using hybrid continuum-discrete element method. *Rock Mech Rock Eng* 49(10):4049–4060
- Indraratna B, Welideniya S, Brown T (2005) A shear strength model for idealised infilled joints under constant normal stiffness 55(3):215–226. <http://works.bepress.com/bindraratna/74>
- Indraratna B, Jayanathan M, Brown T (2008) Shear strength model for overconsolidated clay-infilled idealised rock joints. 58(1):55–65. <http://works.bepress.com/bindraratna/20>
- Khosravi A, Serej AD, Mousavi SM, Haeri SH (2016) Effect of hydraulic hysteresis and degree of saturation of infill materials on the behavior of an infilled rock fracture. *Int J Rock Mech Min Sci* 88:105–114
- Lei Q, Latham JP, Tsang CF (2017) The use of discrete fracture networks for modelling coupled geomechanical and hydrological behaviour of fractured rocks. *Comput Geotech* 85:151–176
- Leung CTO, Zimmerman RW (2012) Estimating the hydraulic conductivity of two-dimensional fracture networks using network geometric properties. *Transp Porous Med* 93(3):777–797
- Li B, Liu R, Jiang Y (2016) Influences of hydraulic gradient, surface roughness, intersecting angle, and scale effect on nonlinear flow behavior at single fracture intersections. *J Hydrol* 538:440–453
- Liu R, Li B, Jiang Y, Huang N (2016a) Review: mathematical expressions for estimating equivalent permeability of rock fracture networks. *Hydrogeol J* 24(7):1623–1649
- Liu R, Li B, Jiang Y (2016b) A fractal model based on a new governing equation of fluid flow in fractures for characterizing hydraulic properties of rock fracture networks. *Comput Geotech* 75:57–68
- Liu R, Li B, Jiang Y (2016c) Critical hydraulic gradient for nonlinear flow through rock fracture networks: the roles of aperture, surface roughness, and number of intersections. *Adv Water Res* 88:53–65
- Lomize GM (1951) Flow in fractured rocks. Gosenergoizdat, Moscow
- Louis C (1969) A study of groundwater flow in jointed rock and its influence on the stability of rock masses. Report at Imperial College of Science and Technology
- Nazridoust K, Ahmadi G, Smith DH (2006) A new friction factor correlation for laminar, single-phase flows through rock fractures. *J Hydrol* 329(1):315–328
- Olsson R, Barton N (2001) An improved model for hydromechanical coupling during shearing of rock joints. *Int J Rock Mech Min Sci* 38(3):317–329
- Patir N, Cheng HS (1978) An average flow model for determining effects of three-dimensional roughness on partial hydrodynamic lubrication. *J Tribol* 100:12–17
- Rasouli V, Hosseini A (2011) Correlations developed for estimation of hydraulic parameters of rough fractures through the simulation of JRC flow channels. *Rock Mech Rock Eng* 44:447–461
- Rutqvist J (2015) Fractured rock stress-permeability relationships from in situ data and effects of temperature and chemical-mechanical couplings. *Geofluids* 15(1–2):48–66. doi:10.1111/gfl.12089
- Song Q, Yanful EK (2010) Effect of channelling on water balance, oxygen diffusion and oxidation rate in mine waste rock with an inclined multilayer soil cover. *J Contam Hydrol* 114(1):43–63
- Song Q, Yanful EK (2011) Laboratory and numerical modeling of water balance in a layered sloped soil cover with channel flow pathway over mine waste rock. *Environ Earth Sci* 62(1):1–17
- Su B, Zhan M, Zhao J (1995) Study on fracture seepage in the imitative nature rock. *Chin J Geotech Eng* 17(5):19–24 (in Chinese)
- Walsh JB (1981) Effect of pore pressure and confining pressure on fracture permeability. *Int J Rock Mech Min Sci* 18(5):429–435
- Wang JJ, Huang SY, Hu JF (2016) Mode II fracture toughness of a clay mixed with sand. *Eng Fract Mech* 165:19–23
- Witherspoon PA, Wang JSY, Iwai K, Gale JE (1980) Validity of cubic law for fluid flow in a deformable rock fracture. *Water Resour Res* 16(6):1016–1024
- Wu W, Li JC, Zhao J (2014) Role of filling materials in a P-wave interaction with a rock fracture. *Eng Geol* 172:77–84
- Xiong X, Li B, Jiang Y, Koyama T, Zhang C (2011) Experimental and numerical study of the geometrical and hydraulic characteristics of a single rock fracture during shear. *Int J Rock Mech Min Sci* 48(8):1292–1302
- Yeo IW, De Freitas MH, Zimmerman RW (1998) Effect of shear displacement on the aperture and permeability of a rock fracture. *Int J Rock Mech Min Sci* 35(8):1051–1070
- Zimmerman RW, Bodvarsson GS (1996) Hydraulic conductivity of rock fractures. *Transp Porous Med* 23(1):1–30